

# Scenario Extraction from a Large Real-World Dataset for the Assessment of Automated Vehicles

Detian Guo<sup>a,b</sup>, Manuel Muñoz Sánchez<sup>a\*</sup>, Erwin de Gelder<sup>b</sup>, Tom P.J. van der Sande<sup>a</sup>

**Abstract**—Many players in the automotive field support scenario-based assessment of automated vehicles (AVs), where individual traffic situations can be tested and, thus, facilitate concluding on the performance of AVs in different situations. Since an extremely large number of different scenarios can occur in real-world traffic, the question is how to find a finite set of relevant scenarios. Scenarios extracted from large real-world datasets represent real-world traffic since real driving data is used. Extracting scenarios, however, is challenging because (1) the scenarios to be tested should ensure the AVs behave safely, which conflicts with the fact that the majority of the data contains scenarios that are not interesting from a safety perspective, and (2) extensive data processing is required, which hinders the utilization of large real-world datasets. In this work, we propose a three-step approach for extracting scenarios from real-world driving data. The first step is data preprocessing to tackle the errors and noise in real-world data. The second step performs data tagging to label actors' activities, their interactions with each other, and their interactions with the environment. Finally, the scenarios are extracted by searching for combinations of tags. The proposed approach is evaluated using data simulated with CARLA and applied to a part of a large real-world driving dataset, i.e., the Waymo Open Motion Dataset (WOMD).

## I. INTRODUCTION

The development of automated vehicles (AVs) is drawing more and more attention from many industries, including the automotive industry, smart cities, and smart mobility. AVs have the potential to improve road capacity, energy efficiency, emissions, and road safety since their introduction will gradually reduce the power from human drivers and avoid crashes resulting from human failure [1]. Although the application of AVs is promising, there are still challenges in the effective validation of AVs to assure that these vehicles behave safely in an extremely large number of real-world driving scenarios [2], [3].

To validate the performance of AVs, much research uses a scenario-based approach [4]–[6]. Properly identified scenarios are crucial for scenario-based assessment since they are directly reflected in the test cases for the assessment [7]. To create a common understanding of the scenario-based assessment, definitions for concepts regarding scenarios and their building blocks, e.g., activities, actors, and events, were proposed in [8]. Layered models were derived for the scenario description, which contains information on environmental conditions, activities of road users (RU), and their

This work was partially supported by SAFE-UP under EU's Horizon 2020 research and innovation programme, grant agreement 861570.

<sup>a</sup>Department of Mechanical Engineering, Eindhoven University of Technology, The Netherlands.

<sup>b</sup>Integrated Vehicle Safety, TNO, Helmond, The Netherlands.

\*Corresponding author: m.munoz.sanchez@tue.nl

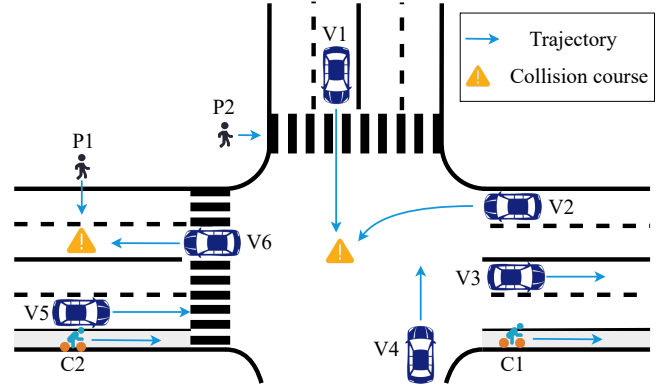


Fig. 1: Overview of the traffic where different RU interact with each other and the environment at a crossroads. Vehicles: V1-V6, pedestrians: P1-P2, cyclists: C1-C2.

interactions [9]–[11]. Previous research regarding scenario identification can be classified as scenario creation based on expert knowledge and scenario extraction from real-world data [12]–[14]. A drawback of scenario creation is that the synthesized scenarios may not be valid or representative of real-world traffic. When using real-world data to extract scenarios for the assessment of AVs, the extracted scenarios are a representation of what an AV might encounter in real-world traffic. In this case, the challenge is the extraction of the relevant, i.e., safety-critical, scenarios from a large amount of data, since the majority of the data contains scenarios that are irrelevant from a safety perspective. For instance, consider the traffic in Fig. 1, where vehicles, pedestrians, and cyclists interact with each other and the environment at a crossroads. Not all interactions in Fig. 1 are relevant for the safety assessment. The extraction of potentially hazardous interactions between two actors, e.g., V1-V2, and P1-V6, is necessary since they are on collision course, whereas interactions V1-P2, V3-V4, and V2-C1, are not extracted since those interactions are not safety critical.

To be representative of real-world traffic, scenario extraction requires a large amount of data, with which it is possible to identify more uncommon scenarios than with small datasets. Recently released large-scale datasets [15]–[18] alleviate the effort of collecting data. However, extracting useful information remains a work that requires extensive data processing. The datasets are usually in large file sizes and hinder their utilization [19], [20].

In this work, we propose an approach to automatically extract scenarios from real driving data with three steps:

data preprocessing, automatic tagging, and searching for the combination of tags based on [21]. We illustrate the proposed approach by extracting scenarios from a large-scale dataset. The contribution of this work is summarized as follows:

- 1) In addition to [21], our tags include not only the activities of RU but also the interaction between each other and the interaction between the RU and the environment. Our tags are suitable for multiple layered models (e.g., [9]–[11]) for the scenario description.
- 2) We evaluate our method using data simulated with CARLA [22], where we have access to the ground truth of scenarios, and we can select the type of scenarios generated. Based on the generated data, we verified that our method correctly extracts the scenarios.
- 3) We provide an open-source library for the scenarios extracted from a large real-world dataset, i.e., the Waymo Open Motion Dataset (WOMD) [17]. This can facilitate the research community to develop and assess automated driving functions (ADFs) in different scenarios.

The remainder of this work is structured as follows. Section II introduces related work on scenario extraction from real-world driving data. Section III presents our scenario extraction methods. Section IV describes the scenarios extracted from simulated data and real-world driving data. This paper ends with conclusions and a discussion on the next steps in Section V.

## II. RELATED WORK

Scenarios are conceptualized using ontologies in [8], [23], [24], which define the basic entities and describe relations among them. The basic entities are actors and environmental elements. Actors are the entities that experience change and can act and react in a scenario [8], [25]. Following this definition, we term road users, e.g., vehicles, cyclists, and pedestrians, as actors. We adopt the term activity from [8], which describes the state change that actors experience in a certain time interval. Environmental elements entail road networks, e.g., crosswalks, and traffic guidance objects, e.g., traffic lights. The relations among the basic entities include the interaction between the actors and the environmental elements and the interaction between different actors.

Next, a selection of previous publications on extracting scenarios from real-world data is introduced. De Gelder and Paardekooper [26] highlight the importance of using scenarios extracted from real-world driving data, since it allows drawing conclusions on the performance of ADFs in real-world traffic. Therefore, this paper focuses on extracting scenarios from real-world driving data.

In [27], lane change scenarios are extracted by comparing vehicles' lane position and lateral distance to the path of the ego vehicle from real-world data. The lane points are clustered into different lanes. Lane changes are detected if any vehicle's lateral displacement to the ego vehicle's lane is less than a threshold.

In [4], detection for turning scenarios with the yaw rate of the car is discussed. The random fluctuations of the estimated

yaw rate are smoothed out with an exponentially decaying weighted averaging filter, which outputs the filtered signal. The turning scenario is detected when the filtered signal crosses a threshold for a certain time interval. This approach, however, can miss quick turns and slow turns where this condition does not hold.

In [21], scenarios are extracted from real-world driving data by labeling the data with tags, e.g., the lateral and longitudinal activities of different actors, and searching for a combination of tags. This approach is efficient since the tags are only detected once and shared while searching for a combination of tags to extract different types of scenarios. The authors determined the longitudinal activities of the actors on highways, e.g., accelerating, decelerating, and cruising, with the speed difference in a certain sample window. The interaction between the ego vehicle and the environment is determined by the location of the ego vehicle based on GPS measurements. We extend this approach with longitudinal tags that are suitable for the urban area, e.g., standing still and reversing.

## III. METHODOLOGY

In this section, we introduce our approach for real-world scenario extraction. As shown in Fig. 2, our approach is abstracted into three steps: data preprocessing, tagging, and scenario categorization. The first step, data preprocessing, is crucial to address inaccuracies in the data. The next step, tagging, is completed by a model-based approach to tag the longitudinal and lateral activities of the actors and their interaction with the environment and each other. The third step, scenario categorization, is to search for the match of predefined scenario categories using a combination of tags. In the following subsections, these three steps are detailed. We assume that the data is in a coordinate frame with the  $x$ -axis pointing to the east and the  $y$ -axis pointing to the north.

### A. Data preprocessing

Despite the benefits brought by publicly released large datasets, noise and missing data in these datasets are inevitable. The reliability of further research without data preprocessing can be influenced [20]. The missing data can stem from a sensor error or an object that is occluded for a certain time interval. To counter this, we linearly interpolate the missing data between the first and the last valid time step. The actor's yaw angle is denoted by  $\psi \in (-\pi, \pi]$ . We compute the yaw rate,  $\omega$ , with Eq. (1), where  $\psi(k)$  denotes the yaw angle at time step  $k$  and  $T_s$  denotes the sampling time.

$$\omega(k+1) = (\psi(k+1) - \psi(k)) / T_s \quad (1)$$

In case  $\psi$  changes from  $\pi$  to  $-\pi$ , or vice versa, we add or subtract  $2\pi T_s$  from  $\omega$  such that  $\omega \in (-\pi T_s, \pi T_s]$ , based on the assumption that the yaw angle change of an actor in a time step is physically restrained. Next, we compute the actor's longitudinal velocity  $v_{\text{long}}$ :

$$v_{\text{long}} = \cos \psi v_x + \sin \psi v_y, \quad (2)$$

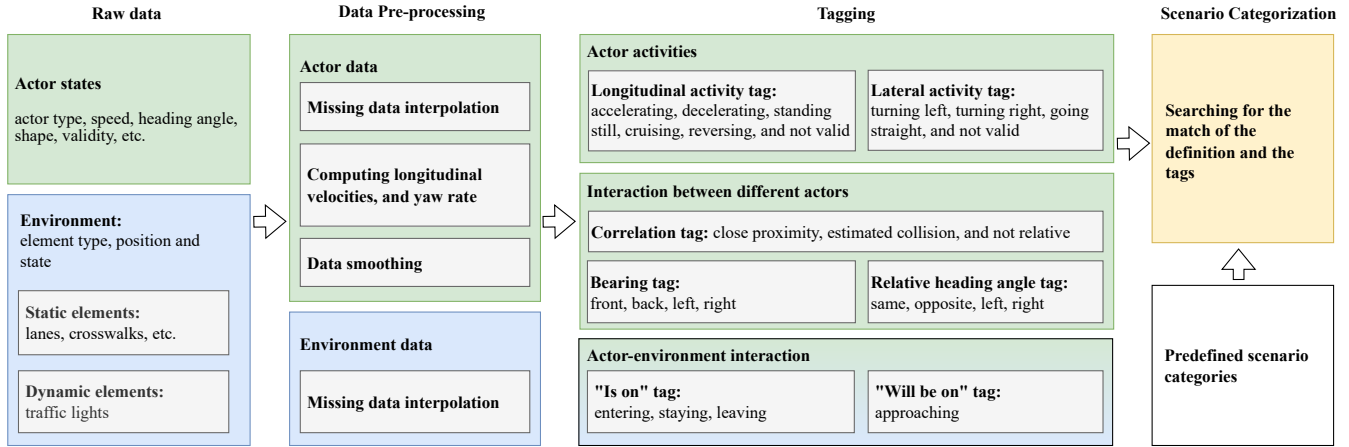


Fig. 2: The three-step approach for scenario extraction from real-world data. The colors green and blue refer to actor-related and environment-related processes and tags, respectively.

where  $v_x$  and  $v_y$  denote the actor's velocities at the  $x$ -axis and the  $y$ -axis, respectively. We utilize cubic splining [28] to smooth the longitudinal velocity.

### B. Tagging

To compose the scenario, we introduce three tag classes: actor activities, actor-environment interaction, and interaction between different actors. Actor activities entail actors' longitudinal and lateral activities, further explained in Section III-B.1. Actor-environment interaction describes how each actor interacts with the environment and is detailed in Section III-B.2. The interaction between different actors in Section III-B.3 comprises the potential hazardous interaction type of two actors. The tag "not valid", which represents the time sequence before the first valid data and after the last valid data, is included in three tag classes.

1) *Actor activity*: Five different types of longitudinal activity tags are distinguished, i.e., "accelerating", "decelerating", "standing still", "cruising", and "reversing". An actor is performing either one of these activities. We use the method in [21] for the tags "accelerating", "decelerating", and "cruising". The following rules are used to tag the activity at the  $k$ -th time step for "reversing" or "standing still" if the condition (3) or (4) holds, respectively:

$$|v_{\text{long}}(k)| T_s \leq \alpha l_{\text{actor}}, \quad (3)$$

$$v_{\text{long}}(k) T_s \leq -\alpha l_{\text{actor}}, \quad (4)$$

where  $v_{\text{long}}$  denotes the longitudinal velocity,  $l_{\text{actor}}$  is the length of the actor's bounding box, and  $\alpha \in (0, 1)$  is a parameter that needs to be set in advance. In this work, we use  $\alpha = 0.01$ .

Lateral activity tags are distinguished into three types, which are "turning left", "turning right", and "going straight". To extract lateral activities, simply checking whether the yaw rate  $\omega$  is above a certain threshold  $\lambda_\omega$  for a certain time interval would miss quick and slow turns. To tackle this problem, we introduce a threshold  $\lambda_\psi$  for

future heading change. Following is the method for detecting "turning left" by using the thresholds  $\lambda_\omega$  and  $\lambda_\psi$ .

- 1) The current time step  $k_c$  is staged as the potential start of "turning left" if the yaw rate is more than  $\lambda_\omega$ :

$$\omega(k_c) > \lambda_\omega. \quad (5)$$

- 2) Determine the nearest end time step  $k_e$  of this lateral activity when the yaw rate is less than  $\lambda_\omega$ , i.e.,

$$\omega(k_e) < \lambda_\omega. \quad (6)$$

- 3) Compare the future heading change with  $\lambda_\psi$ . The lateral activity between  $k_c$  and  $k_e$  is tagged with "turning left" if a certain heading change is achieved, i.e.,

$$T_s \sum_{k=k_c}^{k_e} \omega(k) > \lambda_\psi. \quad (7)$$

We set the threshold for future heading change  $\lambda_\psi = 45^\circ$  based on [29]. Let  $T_d$  denote the longest time interval for a turning activity. Therefore, we define  $\lambda_\omega = \lambda_\psi / T_d$ . The tag "turning right" is detected in a similar manner as "turning left".

2) *Actor-environment interaction*: We investigated the interaction between actors and environmental elements, which is distinguished into five types: "not relative", "approaching", "entering", "staying", and "leaving". For example, the interaction between a crosswalk and a pedestrian that will possibly be on the crosswalk, e.g., P2 in Fig. 1, is tagged with "approaching". This can be vital for the vehicle on the crosswalk, e.g., C1 in Fig. 1, where the interaction of C1 to the crosswalk is subsequently tagged with "entering", "staying", and "leaving". An actor possesses only one tag with one environmental element at each time step. The environmental elements are commonly provided with coordinates of polylines, e.g., lane center, and vertices of polygons, e.g., crosswalks [16], [17]. To detect the tags, we formulate the environmental elements in polygons. We introduce the actual

TABLE I: Rules for generating actor-environment interaction tags.  $\phi_a$ : actual intersection ratio of Eq. (8),  $\phi_e$ : extended intersection ratio,  $\Delta\phi_a$ : the difference of  $\phi_a$  according to Eq. (9).

$\phi_a$	$\phi_e$	$\Delta\phi_a$	Tag
$\phi_a = 0$	$\phi_e = 0$	-	Not relative
$\phi_a = 0$	$\phi_e > 0$	-	Approaching
$\phi_a > 0$	-	$ \Delta\phi_a  \leq 0.01$	Staying
$\phi_a > 0$	-	$\Delta\phi_a > 0.01$	Entering
$\phi_a > 0$	-	$\Delta\phi_a < -0.01$	Leaving

intersection ratio  $\phi_a$  to detect if the actor is “on” the corresponding environmental element. The actual intersection ratio is obtained from the intersection area  $\mathcal{A}_{\text{intersection}}$  of the actor’s bounding box and the environmental element polygon normalized by  $\mathcal{A}_{\text{actor}}$ , which denotes the area of the actor’s bounding box, i.e.,

$$\phi_a = \mathcal{A}_{\text{intersection}} / \mathcal{A}_{\text{actor}}. \quad (8)$$

The normalization facilitates the adaptation of  $\phi_a$  to actors of different sizes. Another indicator used to distinguish the status “on” to tags: “staying”, “entering”, and “leaving” is the difference of the actual intersection ratio  $\Delta\phi_a$  obtained with,

$$\Delta\phi_a = \phi_a(k+1) - \phi_a(k). \quad (9)$$

The tag “approaching” is detected by introducing the extended trajectory polygon  $\mathcal{P}_e$  and the extended intersection ratio  $\phi_e$ . We extend the current actor’s bounding box to the extended trajectory polygon with a constant turn rate and velocity model [30] to extract the actor’s intention to move toward a certain environmental element within a time horizon  $T_e = 3$  s. The method for generating  $\mathcal{P}_e$  is as follows:

- 1) At each time step in  $T_e$ , a sequence of polygons is generated with the constant turn rate and velocity model.
- 2) An extended trajectory polygon is the union of the sequence of polygons in the first step.

The extended intersection ratio  $\phi_e$  is the intersection area of  $\mathcal{P}_e$  and the environmental element normalized by the area of  $\mathcal{P}_e$ .

In Table I, the rules for generating actor-environment interaction tags are summarized. If both  $\phi_a = 0$  and  $\phi_e = 0$ , the actor is not interacting with the environmental element. The tag “approaching” is used if  $\phi_a = 0$  and  $\phi_e > 0$ . If  $\phi_a > 0$ , one of the tags “staying”, “entering”, or “leaving” is applicable, depending on the value of  $\Delta\phi_a$ : “entering” if  $\Delta\phi_a > 0.01$ , “leaving” if  $\Delta\phi_a < -0.01$ , and “staying” otherwise.

3) *Interaction between different actors*: This tag class describes the interaction between different actors. We design this tag class based on two observations. The first observation is that actors do not react to every actor in the field of view; rather, they selectively focus on the key actors whose movements will (potentially) collide with theirs. We use the tag “estimated collision” to label this type of interaction. The

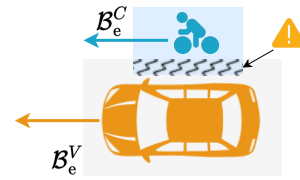


Fig. 3: The expanded bounding boxes  $\mathcal{B}_e^V$  and  $\mathcal{B}_e^C$  for tagging the interactive actors in close proximity.  $C$ : cyclist,  $V$ : vehicle.

second observation stems from the collision hazard with the actors in a nearby neighborhood and the heterogeneity of different actors, such as vehicles, pedestrians, cyclists, etc. For instance, a vehicle and a pedestrian keep a safe distance from each other to avoid a collision while passing by, where the car’s safe distance is considered larger than that of the pedestrian due to the larger shape of the car. We use the tag “close proximity” to label this type of interaction. We term actors tagged with either “close proximity” or “estimated collision” as interactive actors.

The tag “close proximity” is generated by introducing the expanded bounding boxes to adapt to diverse actors’ shapes. Let  $\mathcal{B}_e^i$  denote the expanded bounding box of actor  $i$ . To generate  $\mathcal{B}_e^i$ , the length and width of the original actor’s bounding box are multiplied with a parameter  $\beta = 2$  for expansion. The interaction between actor  $i$  and  $j$  is tagged with “close proximity” when  $\mathcal{B}_e^i$  and  $\mathcal{B}_e^j$  intersect, e.g., Fig. 3.

The tag “estimated collision” is given by introducing the predicted bounding boxes  $\mathcal{B}_p^i$  for an actor  $i$ . At each time instance,  $\mathcal{B}_p^i$  is a sequence of polygons generated with a constant turn rate and velocity model [30], which outputs a time series of the future bounding boxes of the  $i$ -th actor in a prediction time horizon. The actors are tagged with “estimated collision”, e.g., Fig. 4, when the predicted bounding boxes of the actors in any time step of the prediction time horizon overlap with each other, i.e.,

$$\exists k_p \in \{1, \dots, T_p/T_s\}, \text{ s.t. } \mathcal{B}_p^i(k_p) \cap \mathcal{B}_p^j(k_p) \neq \emptyset, \quad (10)$$

where  $\mathcal{B}_p^i(k_p)$  and  $\mathcal{B}_p^j(k_p)$  are the predicted bounding boxes of two different actors at the time step  $k_p$  and  $T_p$  denotes the prediction time horizon. In this work, we use  $T_p = 5$  s. The tag “not relative” is given to two interactive actors at the time instances not tagged with “close proximity” or “estimated collision”. In the remainder of this work, without loss of generality, we term one of two interactive actors as the host actor and the other as the guest actor. Note that the selection of the host and the guest actor is arbitrary.

To describe the interaction of different actors in detail, we further tagged the interactive actors with their relative heading and bearing angles. The relative heading angle is the angle to rotate the heading vector of the host actor to that of the guest actor. The bearing angle is the angle to rotate the heading vector of the host actor to the bearing vector, which points from the center of the host to that of the guest actor. The rules for tagging the relative heading angle and the bearing angle are provided in Table II.

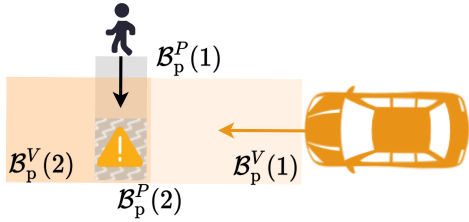


Fig. 4: The predicted bounding boxes  $\mathcal{B}_p^P$  and  $\mathcal{B}_p^V$  for tagging the interactive actors with estimated collision.  $P$ : pedestrian,  $V$ : vehicle,  $\mathcal{B}_p(k_p)$ :  $\mathcal{B}_p$  at the time step  $k_p$ .

TABLE II: Rules of tagging relative heading and bearing angles of actors interacting with each other.

Angle range / rad	Relative heading tag	Bearing tag
$(-\pi, -0.75\pi]$ or $(0.75\pi, \pi]$	Opposite	Back
$(-0.75\pi, -0.25\pi]$	Right	Right
$(-0.25\pi, 0.25\pi]$	Same	Front
$(0.25\pi, 0.75\pi]$	Left	Left

### C. Scenario categorization using tags

We formulate a scenario category using a combination of tags. For example, Table III shows the definition matrix of the scenario category “vehicle-to-cyclist passing by” using tags. In the scenarios that fall in this scenario category, a vehicle and a cyclist are going straight while passing each other closely, and the cyclist is on the left or right side of the vehicle. The scenarios are extracted by searching for matches within the tags, where the logical rules AND, OR, or NOT may be used [21].

## IV. RESULTS

Here we describe the results of our method by applying it to simulated data and real-world driving data. To evaluate our method, the simulated data is generated with the CARLA simulator [22]. Previous studies [4], [21] evaluated their approaches with manually labeled real-world driving data, which is not feasible for large datasets. By using simulated data to evaluate the scenarios, we can customize the environment conditions and traffic flow of the data, where we have access to the ground truth of scenarios, and we

TABLE III: Definition matrix of the scenario category “vehicle-to-cyclist passing by”.

	Host actor tag	Guest actor tag
Actor type	Vehicle	Cyclist
Longitudinal activity	Accelerating OR decelerating OR cruising	Accelerating OR decelerating OR cruising
Lateral activity	Going straight	Going straight
Interaction with the environment	-	-
Interaction between actors	Close proximity	-
Bearing	Left OR right	-
Relative heading	Same	-

TABLE IV: Scenario categories for evaluation and scenario mining.

	Description
SC1	A vehicle is turning left. Another vehicle is going straight in the opposite direction. The two vehicles are on collision course.
SC2	A vehicle and a cyclist are going straight while passing each other closely. The cyclist is on either side of the vehicle.
SC3	A pedestrian is crossing a vehicle’s lane and the pedestrian and vehicle are on collision course.

can select the type of scenarios generated. To evaluate the performance of our approach, we customize the three scenario categories shown in Table IV and record 30 simulated data in different areas, e.g., surface streets, crosswalks, and intersections, where a vehicle interacts with different types of actors. For this experiment, we have used  $T_s = 0.05$  s and  $T_d = 20$  s. Our approach correctly extracts all of the three predefined scenario categories, and no scenarios were incorrectly extracted.

To illustrate the applicability, our approach is applied to the training subset of a large real-world driving dataset, i.e., WOMB [17]. The training subset includes 1,000 data sequences. Each data sequence contains 9.1 s of real-world traffic sampled at 10 Hz, thus we use  $T_s = 0.1$  s and  $T_d = 9.1$  s. The total data used in this paper contains approximately 8.68 million vehicle trajectories, 0.97 million pedestrian trajectories, and 7.78 thousand cyclist trajectories. A challenge with large datasets is that the majority of the data typically contains scenarios that are not interesting from a safety perspective. This is illustrated by the fact that the considered data contains approximately 320 million vehicle-vehicle interactions, 63.85 million vehicle-pedestrian interactions, and 4.34 million vehicle-cyclist interactions. Only a small part of these interactions are considered for the three types of scenarios listed in Table IV.

The three types of scenarios listed in Table IV are extracted, which in total consist of 215,090 scenarios. We randomly examine 116 extracted scenarios with visualizations, e.g., Fig. 5. No examined scenarios are incorrectly extracted. There are approximately 50%, 12%, and 38% of the extracted scenarios that fall in the scenario category SC1, SC2, and SC3, respectively. As a start toward building a real-world scenario database with more scenario categories, we observe an imbalance in the distribution of the three scenario categories. This imbalance can result in misjudgment of data-driven models for ADFs, which are often evaluated by averaging errors over large datasets without scenario distinction [5]. For instance, consider two trajectory prediction models, A and B. Model A is more accurate in SC1, and model B is more accurate in SC2. Given the greater prevalence of SC1 scenarios in the dataset, model A would be deemed superior. However, in areas with heavy cyclist traffic, model B would be preferred. Therefore, it is crucial to consider the operational design domain where ADFs will be deployed and to assess which models are best suited for each specific domain according to the evaluations performed

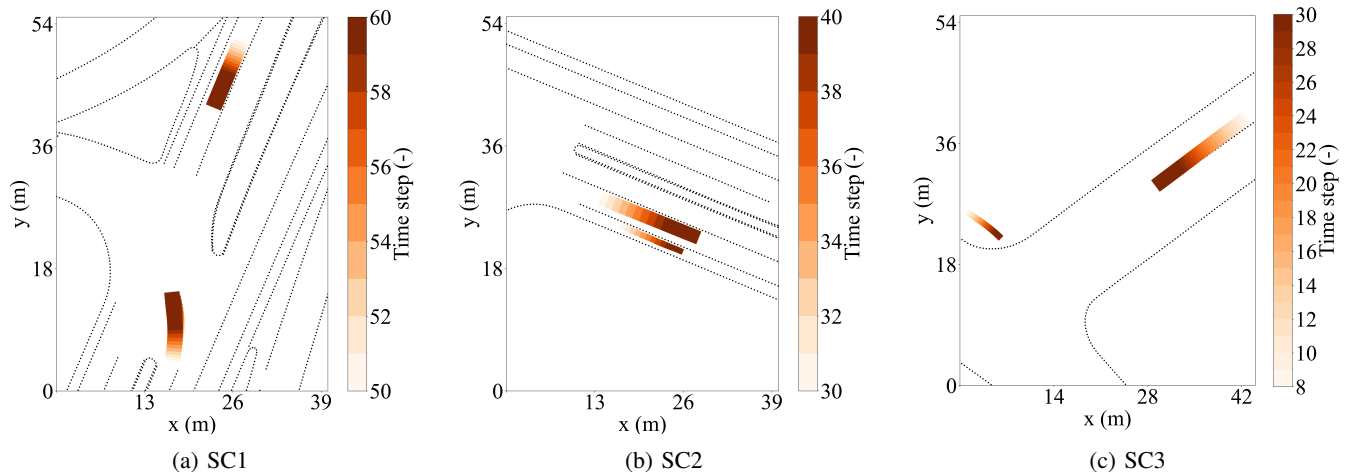


Fig. 5: Examples for the extracted scenarios. The origin of the coordinate system is an arbitrary point.

on the corresponding scenario categories.

We provide an open-source library for the extracted scenarios. The scenarios come with corresponding sample time, scene ID, and actor ID, which align with WOMD, to facilitate the research community to track and understand this large real-world driving dataset.

## V. CONCLUSION AND FUTURE WORK

Scenario identification is crucial for the safety assessment of automated vehicles. In this work, a three-step approach for extracting scenarios from large real-driving datasets is proposed. The first step involves data preprocessing to fill in missing data and reduce noise. The second step performs data tagging. There are three classes of tags: actor activity, actor-environment interaction, and interaction between different actors. The last step extracts the scenarios by searching for a combination of tags.

The approach is evaluated with the data simulated with CARLA [22], where the traffic and the environmental conditions can be customized. By using simulated data, the ground truth of scenarios is accessible, and we can select the type of scenarios generated. The approach is applied to the training subset of a large real-world driving dataset, i.e., WOMD [17]. A total of 215,090 scenarios across three scenario categories are extracted. There is an imbalance in the distribution of the three scenario categories that can result in misjudgment while evaluating data-driven models, where errors are often computed equally among different types of scenarios. The extracted scenarios are open to the research community to gain an understanding of the scenarios contained in WOMD. Future work includes labeling WOMD with more tags and extracting more scenario categories to build a real-world scenario database.

## REFERENCES

- [1] D. Milakis, B. Van Arem, and B. Van Wee, "Policy and society related implications of automated driving: A review of literature and directions for future research," *Journal of Intelligent Transportation Systems*, vol. 21, no. 4, pp. 324–348, 2017.
- [2] H. Watanabe, L. Tobisch, J. Rost, J. Wallner, and G. Prokop, "Scenario Mining for Development of Predictive Safety Functions," in *2019 IEEE International Conference on Vehicular Electronics and Safety (ICVES)*, 2019, pp. 1–7.
- [3] Q. Song, P. Runeson, and S. Persson, "A Scenario Distribution Model for Effective and Efficient Testing of Autonomous Driving Systems," in *37th IEEE/ACM International Conference on Automated Software Engineering*, 2022, pp. 1–8.
- [4] H. Elrofai, D. Worm, and O. Op den Camp, "Scenario Identification for Validation of Automated Driving Functions," in *Advanced Microsystems for Automotive Applications*, 2016, pp. 153–163.
- [5] M. Muñoz Sánchez, J. Elfring, E. Silvas, and R. van de Molengraft, "Scenario-based Evaluation of Prediction Models for Automated Vehicles," in *IEEE International Conference on Intelligent Transportation Systems (ITSC)*, 2022, pp. 2227–2233.
- [6] M. Lesemann, A. Zlocki, J. M. Dalmau, M. Vesco, H. Eriksson, J. Jacobson, and L. Nordström, "A test programme for active vehicle safety – detailed discussion of the eVALUE testing protocols for longitudinal and stability functionality," in *22nd Enhanced Safety of Vehicles (ESV) Conference*, 2011.
- [7] J. E. Stellet, M. R. Zofka, J. Schumacher, T. Schamm, F. Niewels, and J. M. Zollner, "Testing of Advanced Driver Assistance Towards Automated Driving: A Survey and Taxonomy on Existing Approaches and Open Questions," in *IEEE International Conference on Intelligent Transportation Systems (ITSC)*, 2015, pp. 1455–1462.
- [8] E. de Gelder, J.-P. Paardekooper, A. Khabbaz Saberi, H. Elrofai, O. Op den Camp, S. Kraines, J. Ploeg, and B. De Schutter, "Towards an Ontology for Scenario Definition for the Assessment of Automated Vehicles: An Object-Oriented Framework," *IEEE Transactions on Intelligent Vehicles*, vol. 7, no. 2, pp. 300–314, 2022.
- [9] T. Menzel, G. Bagschik, and M. Maurer, "Scenarios for Development, Test and Validation of Automated Vehicles," in *IEEE Intelligent Vehicles Symposium (IV)*, vol. 2018-June, 2018, pp. 1821–1827.
- [10] F. Schuldt, A. Reschka, and M. Maurer, "A Method for an Efficient, Systematic Test Case Generation for Advanced Driver Assistance Systems in Virtual Environments," in *Automotive Systems Engineering II*, 2018, pp. 147–175.
- [11] M. Scholtes, L. Westhofen, L. R. Turner, K. Lotto, M. Schuldes, H. Weber, N. Wagener, C. Neurohr, M. H. Bollmann, F. Kortke, J. Hiller, M. Hoss, J. Bock, and L. Eckstein, "6-Layer Model for a Structured Description and Categorization of Urban Traffic and Environment," *IEEE Access*, vol. 9, pp. 59 131–59 147, 2021.
- [12] J. Cai, W. Deng, H. Guang, Y. Wang, J. Li, and J. Ding, "A Survey on Data-Driven Scenario Generation for Automated Vehicle Testing," *Machines*, vol. 10, no. 11, p. 1101, 2022.
- [13] X. Wang, Y. Peng, T. Xu, Q. Xu, X. Wu, G. Xiang, S. Yi, and H. Wang, "Autonomous driving testing scenario generation based on in-depth vehicle-to-powered two-wheeler crash data in China," *Accident Analysis & Prevention*, vol. 176, p. 106812, 10 2022.
- [14] F. Hauer, I. Gerostathopoulos, T. Schmidt, and A. Pretschner, "Clus-

- tering Traffic Scenarios Using Mental Models as Little as Possible,” in *IEEE Intelligent Vehicles Symposium (IV)*, 2020, pp. 1007–1012.
- [15] H. Caesar, V. Bankiti, A. H. Lang, S. Vora, V. E. Liong, Q. Xu, A. Krishnan, Y. Pan, G. Baldan, and O. Beijbom, “Nuscenes: A multimodal dataset for autonomous driving,” in *IEEE/CVF Conference on Computer Vision and Pattern Recognition (CVPR)*, 2020, pp. 11 618–11 628.
- [16] M.-F. Chang, J. Lambert, P. Sangkloy, J. Singh, S. Bak, A. Hartnett, D. Wang, P. Carr, S. Lucey, D. Ramanan, and J. Hays, “Argoverse: 3D tracking and forecasting with rich maps,” in *IEEE/CVF Conference on Computer Vision and Pattern Recognition (CVPR)*, 2019, pp. 8740–8749.
- [17] S. Ettinger, S. Cheng, B. Caine, C. Liu, H. Zhao, S. Pradhan, Y. Chai, B. Sapp, C. Qi, Y. Zhou, Z. Yang, A. Chouard, P. Sun, J. Ngiam, V. Vasudevan, A. McCauley, J. Shlens, and D. Anguelov, “Large Scale Interactive Motion Forecasting for Autonomous Driving: The WAYMO OPEN MOTION DATASET,” in *IEEE/CVF International Conference on Computer Vision (ICCV)*, 2021, pp. 9690–9699.
- [18] Y. Ma, X. Zhu, S. Zhang, R. Yang, W. Wang, and D. Manocha, “TrafficPredict: Trajectory prediction for heterogeneous traffic-agents,” in *AAAI Conference on Artificial Intelligence*, vol. 33, no. 01, 2019, pp. 6120–6127.
- [19] D. Zhao, Y. Guo, and Y. J. Jia, “TrafficNet: An open naturalistic driving scenario library,” in *IEEE International Conference on Intelligent Transportation Systems (ITSC)*, 2017, pp. 1–8.
- [20] X. Hu, Z. Zheng, D. Chen, X. Zhang, and J. Sun, “Processing, assessing, and enhancing the Waymo autonomous vehicle open dataset for driving behavior research,” *Transportation Research Part C: Emerging Technologies*, vol. 134, p. 103490, 1 2022.
- [21] E. de Gelder, J. Manders, C. Grappiolo, J. P. Paardekooper, O. Op den Camp, and B. De Schutter, “Real-World Scenario Mining for the Assessment of Automated Vehicles,” in *IEEE International Conference on Intelligent Transportation Systems (ITSC)*, 2020.
- [22] A. Dosovitskiy, G. Ros, F. Codevilla, A. López, and V. Koltun, “CARLA: An Open Urban Driving Simulator,” in *the 1st Annual Conference on Robot Learning*, 2017, pp. 1–16.
- [23] S. Geyer, M. Baltzer, B. Franz, S. Hakuli, M. Kauer, M. Kienle, S. Meier, T. Weigerber, K. Bengler, R. Bruder, F. Flemisch, and H. Winner, “Concept and development of a unified ontology for generating test and use-case catalogues for assisted and automated vehicle guidance,” *IET Intelligent Transport Systems*, vol. 8, no. 3, pp. 183–189, 5 2014.
- [24] G. Bagschik, T. Menzel, and M. Maurer, “Ontology based Scene Creation for the Development of Automated Vehicles,” *IEEE Intelligent Vehicles Symposium (IV)*, pp. 1813–1820, 2018.
- [25] ISO 34501, “Road vehicles — Test scenarios for automated driving systems — Vocabulary,” International Organization for Standardization, Tech. Rep., 2022.
- [26] E. de Gelder and J.-P. Paardekooper, “Assessment of Automated Driving Systems using real-life scenarios,” in *IEEE Intelligent Vehicles Symposium (IV)*, 2017, pp. 589–594.
- [27] D. Karunakaran, J. S. Berrio, S. Worrall, and E. Nebot, “Automatic lane change scenario extraction and generation of scenarios in OpenX format from real-world data,” *arXiv preprint arXiv:2203.07521*, 2022.
- [28] C. de Boor, *A Practical Guide to Splines*. Springer, 1 1978, vol. 27.
- [29] E. A. Pool, J. F. Kooij, and D. M. Gavrila, “Using road topology to improve cyclist path prediction,” in *IEEE Intelligent Vehicles Symposium (IV)*, 2017, pp. 289–296.
- [30] R. Schubert, C. Adam, M. Obst, N. Mattern, V. Leonhardt, and G. Wanielik, “Empirical evaluation of vehicular models for ego motion estimation,” in *IEEE Intelligent Vehicles Symposium (IV)*, 2011, pp. 534–539.